HHS Public Access

Author manuscript

Biochimie. Author manuscript; available in PMC 2022 February 01.

Published in final edited form as:

Biochimie. 2021 February ; 181: 25–33. doi:10.1016/j.biochi.2020.11.018.

X-aptamers targeting Thy-1 membrane glycoprotein in pancreatic ductal adenocarcinoma

Hongyu Wang[1,2], **Xin Li**[1], **Lisa A Lai**[3], **Teresa A. Brentnall**[3], **David W. Dawson**[4,5], **Kimberly A. Kelly**[6], **Ru Chen**[7], **Sheng Pan**[1,8]

[1]The Brown Foundation Institute of Molecular Medicine, University of Texas Health Science Center at Houston, Houston, TX 77030, USA

[2]Department of Diagnostic and Interventional Imaging, University of Texas Health Science Center at Houston, Houston, TX 77030, USA

[3]Division of Gastroenterology, Department of Medicine, the University of Washington, Seattle, WA 98195, USA

[4]Department of Pathology and Laboratory Medicine, UCLA, Los Angeles, CA 90095, USA

[5]Jonsson Comprehensive Cancer Center, David Geffen School of Medicine, UCLA, Los Angeles, CA 90095, USA

[6]Department of Biomedical Engineering, University of Virginia School of Engineering and Applied Sciences, Charlottesville, VA 22908

[7]Division of Gastroenterology and Hepatology, Department of Medicine, Baylor College of Medicine, Houston, TX 77030, USA

[8]Department of Integrative Biology and Pharmacology, University of Texas Health Science Center at Houston, Houston, TX 77030, USA

Abstract

Modified DNA aptamers incorporated with amino-acid like side chains or drug-like ligands can offer unique advantages and enhance specificity as affinity ligands. Thy-1 membrane glycoprotein (THY1 or CD90) was previously identified as a biomarker candidate of neovasculature in pancreatic ductal adenocarcinoma (PDAC). The current study developed and evaluated modified DNA X-aptamers targeting THY1 in PDAC. The expression and glycosylation of THY1 in PDAC tumor tissues were assessed using immunohistochemistry and quantitative proteomics. Bead-based

*Correspondence should be addressed to HW (hongyu.wang@uth.tmc.edu) and SP (sheng.pan@uth.tmc.edu).

Author Contributions

HW and SP designed the experiments. HW, LAL, DWD and XL conducted the experiments. HW and SP prepared the original draft. HW, SP, RC, TAB and LAL reviewed and edited the manuscript. SP, TAB, RC, DWD and KAK provided the resources.

Declaration of interests

The authors declare that they have no known competing financial interests or personal relationships that could have appeared to influence the work reported in this paper.

X-aptamer library that contains 10^8 different sequences was used to screen for high affinity THY1 X-aptamers. The sequences of the X-aptamers were analyzed with the next-generation sequencing. The affinities of the selected X-aptamers to THY1 were quantitatively evaluated with flow cytometry. Three high affinity THY1 X-aptamers, including XA-B217, XA-B216 and XA-A9, were selected after library screening and affinity binding evaluation. These three X-aptamers demonstrated a high binding affinity and specificity to THY1 protein and the THY1 expressing cell lines, using THY1 antibody as a comparison. The development of these X-aptamers provides highly specific and non-immunogenic affinity ligands for THY1 binding in the context of biomarker development and clinical applications. They could be further exploited to assist molecular imaging of PDAC targeting THY1.

Keywords

Thy-1 membrane glycoprotein (THY1 or CD90); aptamer; pancreatic cancer; proteomics

1. Introduction

Thy-1 membrane glycoprotein (THY1 or CD90) is an N-glycosylated cell surface protein that is expressed in a variety of tumor cells and normal cell types (e.g., fibroblasts, neurons, and endothelial cells). It can facilitate the attachment of tumor cells to endothelial cells and promote tumor metastasis [1]. In pancreatic ductal adenocarcinoma (PDAC), THY1 has been previously found to be overexpressed in pancreatic tumor tissues, including cancer cells, fibroblasts and vascular endothelial cells [2–4]. It was further evaluated as a molecular target for PDAC detection using the microbubble-enhanced ultrasound imaging technique [5]. More recently, a study exemplified a proof-of-principle approach from engineering a dual human and murine THY1-binding single-chain-antibody ligand to generate contrast microbubbles to allow PDAC detection with ultrasound [6].

Monoclonal antibodies that specifically recognize proteins expressed in cancer cells have been used as homing devices for targeted imaging. However, antibodies are highly immunogenic, and relatively unstable to environmental stress. Especially, antibody can produce high background and has low penetration rate for imaging detection. On the other hand, aptamers can offer complementary advantages such as lower cost, non-immunogenicity [7], and facile modification for various applications [8, 9]. Aptamers are also easier to produce with minimum batch-to-batch variation. At least one aptamer (Macugen) has been approved by the FDA for therapeutic use [10] and several others are in various phases of clinical development for the treatment of diverse medical conditions, such as AMD, acute myeloid leukemia (AML), metastatic renal cell carcinoma, type 2 diabetes mellitus, von Willebrand disease (VMD), thrombosis, heart disease, acute coronary syndrome and hemophilia [11–14]. In addition, aptamers have a wide range of applications for biosensing, disease detection and diagnosis [15–17].

Traditional aptamers developed by using systematic evolution of ligands by exponential enrichment (SELEX) do not possess the binding affinity and specificity required for therapeutic use [18, 19]. While efforts have been made to improve aptamer binding

efficiency, such as to glycoproteins [20–22], modified functionally diverse aptamers that can interact more robustly with targeted proteins hold significant promise for improving the performance of traditional aptamers [8, 23, 24]. We have previously developed DNA X-aptamers (XAs) incorporated with amino-acid like side chains or drug-like ligands (X) to 5-positions of certain uridines on an oligonucleotide backbone [25, 26]. These side chains can convert a modestly binding aptamer to a highly specific and slow-off tight binding X-aptamer, increasing affinity significantly [25]. Based on the modified XAs, a bead-based X-aptamer library that is synthesized by solid phase split-pool method and contains 10^8 different sequences has been created [28–30]. The variety and combination of modifications of the library are far superior to what can be accomplished *via* enzymatic SELEX methods [23–25, 31–33].

In this study, the expression of THY1 in PDAC was examined in cancer and pancreatic intraepithelial neoplasia (PanIN) tissue specimens, as well as multiple PDAC cell lines using proteomics, immunochemistry and flow cytometry. The bead-based modified X-aptamer library was applied to select specific XAs for human THY1 using a two-step process. The next-generation sequencing (NGS) was applied to reveal the sequences of the selected XAs. The specific affinity of the selected XAs was further characterized using flow cytometry and immunochemistry to identify the optimal XA sequences for THY1 binding.

2. Materials and Methods

2.1. Proteomics and glycoproteomics analysis of pancreatic tissues.

The experimental details of the proteomic and glycoproteomic analysis of pancreatic tissue specimens can be found in our previous work [34]. Briefly, snap frozen tissues were homogenized into lysates, and the proteins were reduced with DL-dithiothreitol and alkylated with iodoacetamide. After purification, the proteins were digested with sequencing grade trypsin (Promega, Madison, WI). Equal amounts of digested control and cancer samples were separately labeled with formaldehyde-H2 (light) and formaldehyde-D2 (heavy) (Isotec, Champaign, Illinois), respectively. The light- and heavy-labeled samples were combined and purified through C18 purification columns. A small portion of the sample was preserved for global protein analysis. The rest of the majority sample was oxidized with sodium meta-periodate and incubated with hydrazide resin beads (ThermoFisher Scientific, Waltham, MA) to capture the glycopeptides from the tissue samples. The N-linked glycopeptides were collected after cleavage of the peptides using PNGase F.

The samples were analyzed by an LTQ-Orbitrap hybrid mass spectrometer (ThermoFisher Scientific) coupled with a nano-flow HPLC (Eksigent Technologies, Dublin, CA). The samples were first loaded onto a 1.5 cm trap column (IntegraFrit 100μm, New Objective, Woburn, MA) packed with Magic C18AQ resin (5μm, 200Å particles; Michrom Bioresources, Auburn, CA) with Buffer A (D.I. water with 0.1% formic acid) at a flow rate of 3 μL/minute. The peptide samples were then separated by a 27cm analytical column (PicoFrit 75μm, New Objective) packed with Magic C18AQ resin (5μm, 100Å particles; Michrom Bioresources) followed by mass spectrometric analysis. A 90-minute LC gradient was used as follows: 5% to 7% Buffer B (acetonitrile with 0.1% formic acid) versus Buffer

A over 2 minutes, then to 35% over 90 minutes. The flow rate for the peptide separation was 300 nL /minute. For MS analysis, a spray voltage of 2.25 kV was applied to the nanospray tip. The mass spectrometric analysis was performed using data-dependent acquisition (DDA) with a m/z range of 400–1800, consisting of a full MS scan in the Orbitrap followed by up to 5 MS/MS spectra acquisitions in the linear ion trap using collision induced dissociation (CID). Other mass spectrometer parameters include: isolation width 2 m/z, target value 1e4, collision energy 35%, max injection time 100 ms. Lower abundance peptide ions were interrogated using dynamic exclusion (exclusion time 45 second, exclusion mass width −0.55 m/z low to 1.55 m/z high). Charge state screen was used, allowing for MS/MS of any ions with identifiable charge states +2, +3, and +4 and higher. Raw machine output files of MS/MS spectra were converted to mzXML files and searched with X!Tandem against the Uniprot human protein database. The database search was restricted with the following parameters, including static modifications: carboxamidomethylation on cysteine, light dimethyl labeling on N-terminus and lysine; and dynamic modifications: oxidation on methionine, differential mass between light and heavy dimethyl labeled on N-terminus and lysine, deamidation of asparagines. Peptide identifications were assigned probability by PeptideProphet. Relative quantitation of heavy and light peptide abundance was performed with Xpress version 2.1. Proteins present in sample were inferred using ProteinProphet.

2.2. THY1 proteins and monoclonal antibodies.

Recombinant human THY1 / CD90 Protein (His Tag) were purchased from Sino Biological (Wayne, PA) and used for aptamer identification. Anti-h THY1 (CD90) antibody (clone 5E10) and isotype control mouse IgG1, ƙ were purchased from BioLegend, Inc. (San Diego, CA). CD90 monoclonal Antibody (AF-9) was purchased from Thermo Fisher Scientific. Streptavidin-Phycoerythrin (PE) or Streptavidin-Fluorescein Isothiocyanate (FITC) were used as secondary antibodies for indirect immunofluorescent staining.

2.3. Immunohistochemistry.

The immunohistochemistry (IHC) study of human pancreatic tissues was approved by the Institutional Review Boards at the University of Washington, UCLA and University of Virginia. The specimens in the tissue microarray were de-identified. IHC analysis of THY1 expression was performed in pancreatic tissue obtained from 24 normal pancreatic tissues, 4 PanIN 1, 11 PanIN 2, 14 PanIN 3, and 12 PDAC. Consecutive tissue sections were stained for the vascular endothelial cell marker CD31 and for human THY1 as previously described [5]. Vascular endothelial cell staining of THY1 was scored with a semi-quantitative IHC score from 0 to 3+ as previously described. In brief, cases with THY1-staining of less than 5%, 5–32%, 33–67%, and greater than 67% of CD31 positive vessels were scored as 0, 1+, 2+, and 3+, respectively.

2.4. Aptamer selection and next-generation sequencing (NGS).

Standard solvents and reagents were purchased from either Sigma-Aldrich, Chemgenes or Alfa Aesar. The XA library was obtained from AM Biotechnologies (Houston, TX, USA). A detailed selection protocol is available from their website (http://www.am-biotech.com/). In order to ensure appropriate folding of the oligonucleotide structure, the XA bead-based library was heated at 95 °C for 5 min and cooled at room temperature for 30 min.

Recombinant human THY1 proteins was labeled with biotin (EZ-Link NHS-PEG4-Biotin, Thermo Pierce). After negative selection with BSA, unbound XA library beads were incubated with biotinylated human THY1 protein for 90 min at room temperature with rotation. Beads carrying XAs bound to protein were recovered by pull-down using streptavidin magnetic particles. The oligonucleotides were cleaved from the library beads by a strong base (50 μl 1M NaOH, at 65 °C for 30 min) and the reaction was neutralized using 40 μl 2M TrisHCl. After pelleting the magnetic particles using a magnetic stand, the solution pool containing XAs was fractionated per the selection protocol and incubated with the biotinylated protein for the second selection step. XA oligonucleotides that bound to human THY1 protein were enriched and isolated after the second binding step according to the XA selection protocol, and then amplified into unmodified oligonucleotides by PCR. The sequences were prepared using the Ion Plus Fragment Library Kit for the Ion Torrent™ Personal Genome Machine™ (PGM) System next-generation sequencing. The sequencing data were processed using Aptaligner© software [35]. Sequences with high frequency of occurrence from target fraction pulldowns over the starting oligonucleotide pool as well as a magnetic particle only control were selected. The selected XAs (XA-THY1) that specifically bind to human THY1 proteins were synthesized with 5′-biotinylation.

2.5. Cell lines and cell binding assay.

Human pancreatic cell lines were screened for THY1 expression using anti-h THY1 (CD90) antibody. Based on varying levels of THY1 expression, HPNE, PANC-1, MIA-PaCa and S2–013 cells were used for X-aptamer cell binding study. Cells were maintained in DMEM medium (HPNE, PANC-1, MIA-PaCa, S2–013) supplemented with 10 % fetal bovine serum (FBS) and 1 % penicillin-streptomycin solution (tissue culture reagents purchased from Life Technologies, NY). All experiments were performed at 70–80 % cell confluence with 5 % CO_2 at 37 °C. The cells were seeded in chamber slides (Cole-Parmer, IL) and incubated with the biotinylated XA-THY1 at different concentrations and cell ratios after blocking with universal blocking buffer (Thermo Fisher Scientific, IL). The binding of the XAs to associated cell lines was measured by fluorescence intensity after incubating with streptavidin fluorescein isothiocyanate (FITC) or streptavidin-phycoerythrin (PE). Non-THY1 expression liver cancer cell line Hep3B were used as negative control.

HUVEC cells (#CRL-1730) were obtained from ATCC. Cells were cultured on gelatin-coated flasks/dishes. Flasks/Dishes were incubated with 0.1% gelatin at 37°C for 60 min and rinsed gently with fresh media to remove excess gelatin. Cells were maintained in F-12K Media (ATCC #30–2004) with the addition of 0.1 mg/ml heparin, 0.03–0.05 mg/ml endothelial cell growth supplement, and 10% fetal bovine serum. For induction of Thy1, HUVEC cells were incubated with 50 ng/ml Phorbol 12-myristate 13-acetate (PMA) or 50 ng/ml Phorbol 12,13-dibutyrate (PDBu) (Sigma).

2.6. Aptamer flow cytometry.

HPNE cells were blocked with universal blocking buffer before incubation with XA-THY1, or scrambled control aptamer at 37 °C for 1 hour. After washing to remove excess XAs, fluorescein-labeled streptavidin (BioLegend, CA) were incubated with cells for 30 min at room temperature. Binding of XA to THY1 expression HPNE cells were measured by

percentage of positive cells and fluorescence intensity with FACScalibur flow cytometry (BD Biosciences, San Jose, CA). Anti-human THY1 antibody (BioLegend, CA) was used as positive controls. The equilibrium dissociation constant (Kd) was obtained by fitting the dependence of mean fluorescence intensity of specific binding on the concentration of the XA to the equation of Y = Bmax X/(Kd + X) using GraphPad Prism for nonlinear regression, single binding site curve fitting.

2.7. Filter binding assay.

Considering the common models developed to calculate the equilibrium dissociation constant (Kd) for aptamers [36–38], we also verified the equilibrium binding constants of our selected XAs for THY1 protein by filter binding assay. The biotinylated XAs (15 nM) were incubated with varying concentrations of THY1 in 10 μL of 20 mM Tris buffer (150 mM NaCl, pH 8.0) for 2 hours at room temperature. After incubation samples were diluted to 100 μL with Tris buffer, transferred to the dot-blot apparatus and filtered under vacuum onto nitrocellulose membranes, which retain the THY1 with any bound XAs. The amount of biotinylated XA retained at each spot was determined by chemiluminescent detection using the Chemiluminescent Nucleic Acid Detection Module (Thermo Scientific) following the manufacturer's instructions. The chemiluminescent signals were collected on a Chemimager (Alpha Innotech). Image analysis and quantification of spot intensities were performed using ImageJ (version 1.53c) [39]. Binding analysis was based on the spot intensities on the nitrocellulose membranes with subtraction of background intensity from all the data points. Saturation binding curves were generated by using GraphPad Prism with curve fits assuming a single binding site. Using nonlinear regression, the equilibrium dissociation constants, Kd, were calculated from the equation Y= Bmax X/(Kd + X), assuming a single binding site.

3. Results

3.1. Expression of THY1 in PDAC tissue specimens.

Proteomic analysis of PDAC tissues in comparison of normal pancreas indicated a significant increase of THY1 expression, as well as a substantially elevated N-linked glycosylation level on two glycosylation sites of THY1 in PDAC (Figure 1). These two N-linked glycosylation motifs, with the unique consensus Asn-X-Ser/Thr sequence (X can be any amino acid except proline) [40], are located at position 42 and 119 in THY1 sequence. Additional potential glycosylation site at position 79 was not mapped due to the short tryptic peptide sequence that contains this site.

Compared to vascular endothelial growth factor receptor (KDR or VEGFR2), which is a well-known signaling protein involved in angiogenesis, IHC vascular staining of THY1 on PDAC showed a significant improved detection of cancer compared to KDR. Ten out of 12 PDAC samples had positive staining using THY1, whereas the KDR staining were positive on 6 out of 12 specimens (Figure 2A). We also tested THY1 vascular expression on Pancreatic Intraepithelial Neoplasia (PanIN) specimens, which are precursor lesions of PDAC. PanIN-3 lesion is carcinoma in situ, the immediate precursor lesion before PDAC, and a critical stage for early detection and intervention of PDAC. As indicated in Figure 2B, THY1 staining increased substantially in the specimens from the patients with PanIN-2 and

PanIN-3 diseases, suggesting a possible implication of THY1 in the early development of pancreatic malignancy. To substantiate these observations on clinical specimens, we used angiogenesis stimulus PDBu to activate HUVECs (Human Umbilical Vein Endothelial Cells), and compared THY1 expression in PDBu-stimulated HUVEC to non-stimulated HUVECs. As indicated in Figure 2C, THY1 expression was dramatically elevated after PDBu stimulation, suggesting that THY1 expression in endothelial cells might be relevant to angiogenesis. Protein network analysis indicates that THY1 participates in various molecular activities of tumorigenesis, including angiogenesis, cell adhesion and immune-response, and interacts with other PDAC associated proteins with relevant molecular functions, including CEACAM5, VEGFA, PECAM1, KDR and ENG (Supplemental Figure 1).

3.2. Screening of THY1 expression level in pancreatic cancer cell lines.

A panel of four pancreatic cancer cell lines and one liver cancer cell line Hep3B with varying degrees of malignancy and genetic complexity were screened for the expression level of THY1 using human THY1 antibody. Flow cytometry analysis was performed by analyzing percentage of cells expressing THY1 protein. We discovered that 99% of HPNE cells express THY1, while other cell lines have various level of THY1 expression, from 90.2% of PANC-1 cells, 1.30% of S2–013, 66.6% of MIA PaCa-2 (Figure 3), to 0.68% of Hep3B (data not shown). Therefore, we used HPNE as THY1 positive cell line for downstream assays. The HPNE cells was developed from human pancreatic duct by transduction with a retroviral expression vector (pBABEpuro) containing the hTERT gene. The hTERT-HPNE cells displayed similar properties as intermediary cells from acinar-to-ductal metaplasia.

3.3. Selection of human THY1 specific X-aptamers and next-generation sequencing (NGS).

The single-cycle XA selection process was performed in two straightforward selection steps as previously described and demonstrated in (Figure 4). Specifically, THY1 protein was labeled with biotin and coupled with streptavidin magnetic beads, and then incubated with X-aptamer library (10^8 different DNA sequences). XAs bound to protein were recovered by magnetic pulldown and separated from beads by a strong base. The solution pool containing XAs was fractionated and incubated with the biotinylated THY1 protein for second step solution selection following the same procedure. The XAs enriched after the second binding step were amplified into unmodified oligonucleotides by PCR. The sequencing was carried out using the Ion Plus Fragment Library Kit for next-generation sequencing. The sequences of the selected XAs were analyzed by Ion Torrent™ Personal Genome Machine™ (**PGM**) System. The sequencing data were processed using Aptaligner© software [35]. Sequences with high frequency of occurrence from target fraction pull downs over the starting oligonucleotide pool as well as a magnetic particle only control were selected. By knowing when the various modifications are added in the base sequence, it is possible to decode any sequence from the library to determine the locations of the chemical modifications. Six human THY1 specific XA sequences were selected for validation on cells (Table 1). The structure and linkage chemistry of X, Y, W to the 5-position of uridine bases are presented in Figure 5.

3.4. Validation of selected XA-THY1s.

Based on NGS results, the top six XA sequences for target protein were synthesized individually and used to determine their binding affinity and specificity. HPNE cells that express high level of THY1 (>99%) were used for testing XAs binding affinity using THY1 antibody as a positive control. A scrambled XA was used as negative control. The binding affinity of the selected XAs to HPNE cells was examined by fluorescence microscopy and determined by fluorescence intensity. Among the six XAs, XA-A9, XA-B216 and XA-B217 demonstrated higher fluorescence intensity and were selected for downstream analysis (Figure 6).

Flow cytometry analysis further indicated that XA-A9 (95%), XA-B216 (92%) and XA-B217 (90%) have high binding affinity and specificity to the THY1 expressing HPNE cells, using THY1 antibody (98%) and scrambled aptamer control (1%) as comparisons (Figure 7A). The binding affinities of the XA-A9, XA-B216 and XA-B217 were also examined using other pancreatic cancer cell lines, including PANC-1, MIA PaCa-2 and S2–013 cells. The selected XAs bound to PANC-1 (XA-A9: 88%, XA-B216: 88%, XA-B217: 91%) (Figure 7B) and MIA PaCa-2 cells (XA-A9: 71%, XA-B216: 62%, XA-B217:70%) (Figure 7C) at a similar binding level compared to THY1 antibody. No binding was observed with S2–013 cells for those selected XAs (Figure 7D).

3.5. The dissociation constant Kd's of selected XAs.

To quantitatively evaluate the binding affinity of the selected XAs, filter-binding methods were performed with the three XAs that showed binding to the THY1 expression cells. All three XAs, XA-A9, XA-B216 and XA-B217, showed strong binding to THY1 protein. The saturation binding curves are shown in Figure 8A. The equilibrium dissociation constants, Kd, were derived from these curves and are determined as XA-A9=15 nM, XA-B216=36 nM and XA-B217=2 nM, respectively (Figure 8A). XA-B217 bound to the THY1 with the highest affinity, while XA-A9 and XA-B216 showed similar binding affinity towards THY1 protein. Furthermore, the binding affinity of those selected XAs was evaluated with THY1 expression cells. HPNE cells were incubated with the XAs at various concentrations and analyzed by flow cytometry. The binding affinity of the XAs was determined by mean fluorescence intensity. Saturation curves were fit from these data, and the dissociation constant Kd values were determined to be XA-A9=77 nM, XA-B216=139 nM and XA-B217=57 nM, respectively (Figure 8B). To confirm the specificity of our XAs, we tested the binding of a random oligonucleotide to THY1. This random oligonucleotide failed to bind to the recombinant THY1 protein. MFold-predicted secondary structures indicated that all selected XA sequences can form hairpin loop structures with the random region forming the loop (Figure 8C).

4. Discussion

We initially discovered overexpression of THY1 in PDAC tissues through proteomic analysis. Validation by tissue microarray showed a significant elevation of THY1 on the neovasculature of human PDAC compared to chronic pancreatitis and normal pancreas. The

association of THY1 expression with pancreatic cancer progression suggests the potential of THY1 as a diagnostic biomarker or therapeutic target in early pancreatic malignancy.

With the advances in aptamer development, we applied modified X-aptamer technology to develop THY1 specific affinity reagent. The XA library has about 1 X 10^8 beads, each bead carrying about 3 X 10^3 copies of a potential XA consisting of a unique chemically modified strand of DNA. Each XA candidate can include a combination of many natural and modified nucleotides. The XA libraries can incorporate modifications that are not compatible with enzymatic incorporation such as phosphorodithioate modification [27, 31, 33, 41–49]. XA libraries can also accommodate combinations of different modifications such as multiple different modified versions of dU as previously described [28]. Any chemical modifications can be used in this process at any number of sites, as long as the modification does not prevent determination of the underlying base sequence [50, 51]. This extensive chemical diversity enables robust interaction with a target improving specificity. For THY1 aptamer development, it is notable that THY1 is a small protein that is heavily glycosylated, and the structure and physiological function of THY1 are influenced by its glycosylation forms. For this concern, we specifically select human THY1 protein as our target for X-aptamer selection.

Using the bead-based XA library originally developed by Yang and others [50], we have identified chemically modified DNA aptamers that can specifically bind to human THY1 protein. The three most highly enriched aptamers, XA-A9, XA-B216 and XA-B217, were identified and synthesized with proper modifications. Their binding affinity and specificity were verified with the THY1 expressing HPNE cells, as well as PANC-1 and MIA PaCa-2 pancreatic cancer cell lines. Compared to human THY1 antibodies, XA-B217, XA-B216 and XA-A9 demonstrated similar cell binding specificity and intensity. Comparing the equilibrium dissociation constants Kds obtained from the protein based filter binding assay and THY1 expression cells based flow cytometry assay, the binding affinities of modified X-aptamers to the targeted recombinant proteins were consistently higher than that to the cells. This is largely due to the fact that proteins in free form have less steric hindrance for binding, and their conformation in solution is different from their conformation in live cells. In this study, our goal is to use the selected aptamers to target THY1 in pancreatic cancers *in vivo*. For these reasons, we chose to validate the binding affinity of X-aptamers using THY1 expressing pancreatic cancer cells directly. The development of XA-B217, XA-B216 and XA-A9 aptamers provides highly specific and non-immunogenic affinity ligands for THY1 binding in the context of biomarker development and clinical application.

Supplementary Material

Refer to Web version on PubMed Central for supplementary material.

Acknowledgements

This work was supported in part with the startup fund to SP provided by the Brown Foundation Institute of Molecular Medicine at University of Texas Health Science Center at Houston (UTHealth) and federal fund from the National Institutes of Health under grant R01CA180949 (RC, SP and TAB). The authors are also grateful for the supports from Canary Foundation (TAB, RC, DWD, KAK and SP) and Walters Foundation for early detection of pancreatic cancer (TAB and LAL), as well as the Clinical and Translational Proteomics Center at UTHealth.

References

1. Saalbach A, et al., The Thy-1/Thy-1 ligand interaction is involved in binding of melanoma cells to activated Thy-1- positive microvascular endothelial cells. Microvasc Res, 2002 64(1): p. 86–93. [PubMed: 12074634]
2. Hermann PC, et al., Distinct populations of cancer stem cells determine tumor growth and metastatic activity in human pancreatic cancer. Cell Stem Cell, 2007 1(3): p. 313–23. [PubMed: 18371365]
3. Pan S, et al., Proteomics portrait of archival lesions of chronic pancreatitis. PLoS One, 2011 6(11): p. e27574. [PubMed: 22132114]
4. Zhu J, et al., Overexpression of CD90 (Thy-1) in pancreatic adenocarcinoma present in the tumor microenvironment. PLoS One, 2014 9(12): p. e115507. [PubMed: 25536077]
5. Foygel K, et al., Detection of pancreatic ductal adenocarcinoma in mice by ultrasound imaging of thymocyte differentiation antigen 1. Gastroenterology, 2013 145(4): p. 885–894 e3. [PubMed: 23791701]
6. Abou-Elkacem L, et al., Thy1-Targeted Microbubbles for Ultrasound Molecular Imaging of Pancreatic Ductal Adenocarcinoma. Clin Cancer Res, 2018 24(7): p. 1574–1585. [PubMed: 29301827]
7. Gilboa E, Berezhnoy A, and Schrand B, Reducing Toxicity of Immune Therapy Using Aptamer-Targeted Drug Delivery. Cancer Immunol Res, 2015 3(11): p. 1195–200. [PubMed: 26541880]
8. Rohloff JC, et al., Nucleic Acid Ligands With Protein-like Side Chains: Modified Aptamers and Their Use as Diagnostic and Therapeutic Agents. Mol Ther Nucleic Acids, 2014 3: p. e201. [PubMed: 25291143]
9. Keefe AD and Cload ST, SELEX with modified nucleotides. Curr Opin Chem Biol, 2008 12(4): p. 448–56. [PubMed: 18644461]
10. Ng EW, et al., Pegaptanib, a targeted anti-VEGF aptamer for ocular vascular disease. Nat Rev Drug Discov, 2006 5(2): p. 123–32. [PubMed: 16518379]
11. Nimjee SM, Rusconi CP, and Sullenger BA, Aptamers: an emerging class of therapeutics. Annu Rev Med, 2005 56: p. 555–83. [PubMed: 15660527]
12. Keefe AD, Pai S, and Ellington A, Aptamers as therapeutics. Nat Rev Drug Discov, 2010 9(7): p. 537–50. [PubMed: 20592747]
13. Adachi T and Nakamura Y, Aptamers: A Review of Their Chemical Properties and Modifications for Therapeutic Application. Molecules (Basel, Switzerland), 2019 24(23): p. 4229.
14. Kaur H, et al., Aptamers in the Therapeutics and Diagnostics Pipelines. Theranostics, 2018 8(15): p. 4016–4032. [PubMed: 30128033]
15. Solhi E and Hasanzadeh M, Critical role of biosensing on the efficient monitoring of cancer proteins/biomarkers using label-free aptamer based bioassay. Biomed Pharmacother, 2020 132: p. 110849. [PubMed: 33068928]
16. Bakhtiari H, et al., Aptamer-based approaches for in vitro molecular detection of cancer. Res Pharm Sci, 2020 15(2): p. 107–122. [PubMed: 32582351]
17. Moutsiopoulou A, et al., Molecular Aptamer Beacons and Their Applications in Sensing, Imaging, and Diagnostics. Small, 2019 15(35): p. e1902248. [PubMed: 31313884]
18. Yang X and Gorenstein DG, Progress in thioaptamer development. Curr. Drug Targets, 2004 5(8): p. 705–15. [PubMed: 15578951]
19. Yang X, Li N, and Gorenstein DG, Strategies for the discovery of therapeutic aptamers. Expert Opin Drug Discov, 2011 6(1): p. 75–87. [PubMed: 21359096]
20. Nie H, et al., Efficient selection of glycoprotein-binding DNA aptamers via boronate affinity monolithic capillary. Anal Chem, 2013 85(17): p. 8277–83. [PubMed: 23895515]
21. Ma Y, et al., Glycan-Imprinted Magnetic Nanoparticle-Based SELEX for Efficient Screening of Glycoprotein-Binding Aptamers. ACS Appl Mater Interfaces, 2018 10(47): p. 40918–40926. [PubMed: 30379519]
22. Li X, et al., Hybrid Approach Combining Boronate Affinity Magnetic Nanoparticles and Capillary Electrophoresis for Efficient Selection of Glycoprotein-Binding Aptamers. Anal Chem, 2016 88(19): p. 9805–9812. [PubMed: 27579807]

23. Gawande BN, et al., Selection of DNA aptamers with two modified bases. Proc Natl Acad Sci U S A, 2017 114(11): p. 2898–2903. [PubMed: 28265062]
24. Gelinas AD, et al., Crystal structure of interleukin-6 in complex with a modified nucleic acid ligand. J Biol Chem, 2014 289(12): p. 8720–34. [PubMed: 24415767]
25. He W, et al., X-aptamers: a bead-based selection method for random incorporation of druglike moieties onto next-generation aptamers for enhanced binding. Biochemistry, 2012 51(42): p. 8321–3. [PubMed: 23057694]
26. Wang H, et al., Selection of PD1/PD-L1 X-Aptamers. Biochimie, 2018 145: p. 125–130. [PubMed: 28912094]
27. Wu SY, et al., 2'-OMe-phosphorodithioate-modified siRNAs show increased loading into the RISC complex and enhanced anti-tumour activity. Nat Commun, 2014 5: p. 3459. [PubMed: 24619206]
28. Lokesh GL, et al., X-Aptamer Selection and Validation. Methods Mol Biol, 2017 1632: p. 151–174. [PubMed: 28730438]
29. Yang X, et al., Immunofluorescence assay and flow-cytometry selection of bead-bound aptamers. Nucleic Acids Res, 2003 31(10): p. e54. [PubMed: 12736320]
30. Yang X., et al., Construction and selection of bead-bound combinatorial oligonucleoside phosphorothioate and phosphorodithioate aptamer libraries designed for rapid PCR-based sequencing. Nucleic Acids Res, 2002 30(23): p. e132. [PubMed: 12466564]
31. Abeydeera ND, et al., Evoking picomolar binding in RNA by a single phosphorodithioate linkage. Nucleic Acids Res, 2016 44(17): p. 8052–64. [PubMed: 27566147]
32. Lou X, Egli M, and Yang X, Determining Functional Aptamer-Protein Interaction by Biolayer Interferometry. Curr Protoc Nucleic Acid Chem, 2016 67: p. 7 25 1–7 25 15.
33. Pallan P, et al., Crystal structure, stability and Ago2 affinity of phosphorodithioate-modified RNAs. RSC Adv, 2014 4(110): p. 64901–64904.
34. Pan S, et al., Quantitative glycoproteomics analysis reveals changes in N-glycosylation level associated with pancreatic ductal adenocarcinoma. J Proteome Res, 2014 13(3): p. 1293–306. [PubMed: 24471499]
35. Lu E, et al., Aptaligner: automated software for aligning pseudorandom DNA X-aptamers from next-generation sequencing data. Biochemistry, 2014 53(22): p. 3523–5. [PubMed: 24866698]
36. Jing M and Bowser MT, Methods for measuring aptamer-protein equilibria: a review. Anal Chim Acta, 2011 686(1–2): p. 9–18. [PubMed: 21237304]
37. Zhang Z, Oni O, and Liu J, New insights into a classic aptamer: binding sites, cooperativity and more sensitive adenosine detection. Nucleic Acids Res, 2017 45(13): p. 7593–7601. [PubMed: 28591844]
38. Mears KS, M.D.L., Ogunjimi O, Whelan RJ, Experimental and mathematical evidence that thrombin-binding aptamers form a 1 aptamer:2 protein complex. Aptamers, 2018 2: p. 64–73.
39. Schneider CA, Rasband WS, and Eliceiri KW, NIH Image to ImageJ: 25 years of image analysis. Nat Methods, 2012 9(7): p. 671–5. [PubMed: 22930834]
40. Bause E, Structural requirements of N-glycosylation of proteins. Studies with proline peptides as conformational probes. Biochem J, 1983 209(2): p. 331–6. [PubMed: 6847620]
41. Yang X, Solid-phase synthesis of oligodeoxynucleotide analogs containing phosphorodithioate linkages. Curr. Protoc. Nucleic Acid Chem, 2016(66): p. 4.71.1–4.71.14.
42. Yang X, Introducing 2'-OMe-thiophosphoramidites. Glen Research, 2015 27(2): p. 4–5.
43. Yang X, et al., Gene Silencing Activity of siRNA Molecules Containing Phosphorodithioate Substitutions. ACS Chem. Biol, 2012 7(7): p. 1214–20. [PubMed: 22512638]
44. Yang X, et al., New Reagents for Synthesis of High Potency siRNA, in TIDES Research, Technology and Product Development. 2011: Boston.
45. Yang X, Thiophosphoramidites and their use in synthesizing oligonucleotide phosphorodithioate linkages. Glen Research, 2008 20(1): p. 4–6.
46. Fennewald SM, et al., Thioaptamer decoy targeting of AP-1 proteins influences cytokine expression and the outcome of arenavirus infections. J. Gen. Virol, 2007 88(Pt 3): p. 981–90. [PubMed: 17325372]

47. Yang X, et al., Selection of thioaptamers for diagnostics and therapeutics. Ann. N. Y. Acad. Sci, 2006 1082: p. 116–119. [PubMed: 17145932]

48. Wang H, et al., Identification of proteins bound to a thioaptamer probe on a proteomics array. Biochem. Biophys. Res. Commun, 2006 347(3): p. 586–93. [PubMed: 16842751]

49. Yang X, et al., Aptamers containing thymidine 3'-O-phosphorodithioates: synthesis and binding to nuclear factor-kappaB. Bioorg. Med. Chem. Lett, 1999 9(23): p. 3357–62. [PubMed: 10612599]

50. Yang X, et al., Construction and selection of bead-bound combinatorial oligonucleoside phosphorothioate and phosphorodithioate aptamer libraries designed for rapid PCR-based sequencing. Nucleic Acids Res, 2002 30(23): p. e132. [PubMed: 12466564]

51. Yang X, Solid-Phase Synthesis of Oligodeoxynucleotide Analogs Containing Phosphorodithioate Linkages. Curr Protoc Nucleic Acid Chem, 2016 66: p. 4 71 1–4 71 14. [PubMed: 27584703]

Highlights

- The expression and glycosylation of Thy-1 membrane glycoprotein (THY1) was examined in PDAC and pancreatic intraepithelial neoplasia (PanIN) tissue specimens, as well as multiple PDAC cell lines.
- Specific X-Aptamers were identified for THY1 using a bead-based X-aptamer library containing several different chemical modifications.
- THY1 X-aptamers were synthesized and their binding affinities and specificities were validated with recombinant THY1 protein and different PDAC cell lines.
- The development of these THY1 aptamers provides highly specific and non-immunogenic affinity ligands for potential applications in pancreatic cancer diagnosis and prognosis.

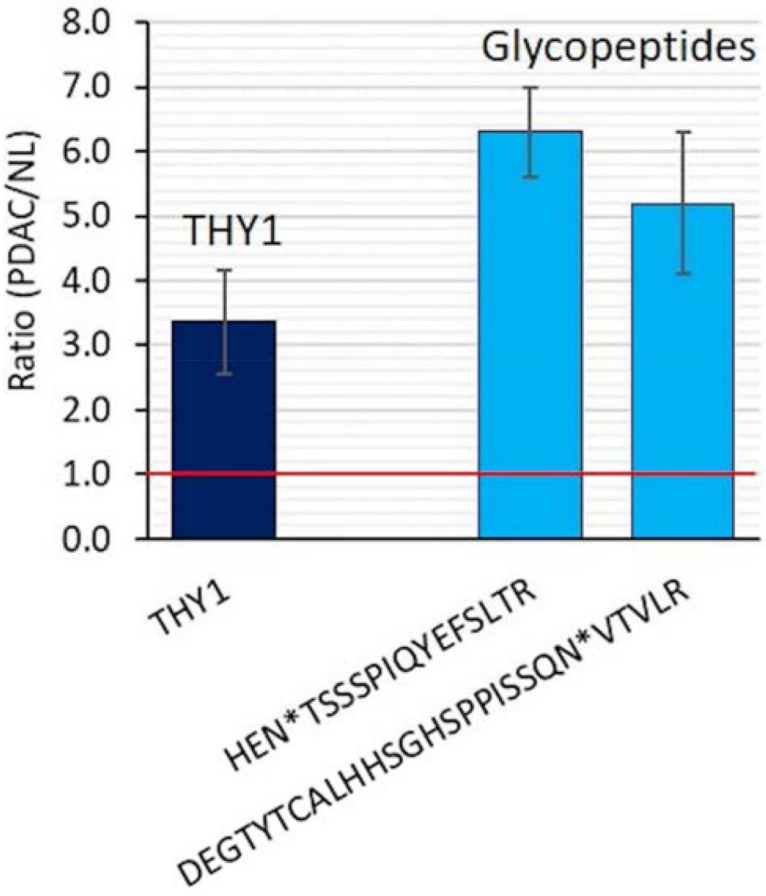

Figure 1.

THY1 expression and N-linked glycosylation in PDAC tissues indicated by proteomics. THY1 was overexpressed (the left bar) and heavily glycosylated on N-linked glycosylation sites (the two right bars) in PDAC tissues compared to normal controls. The two blue bars on the right represent the changes in abundance of the glycopeptides derived from THY1 in PDAC tissue compared to normal pancreas.

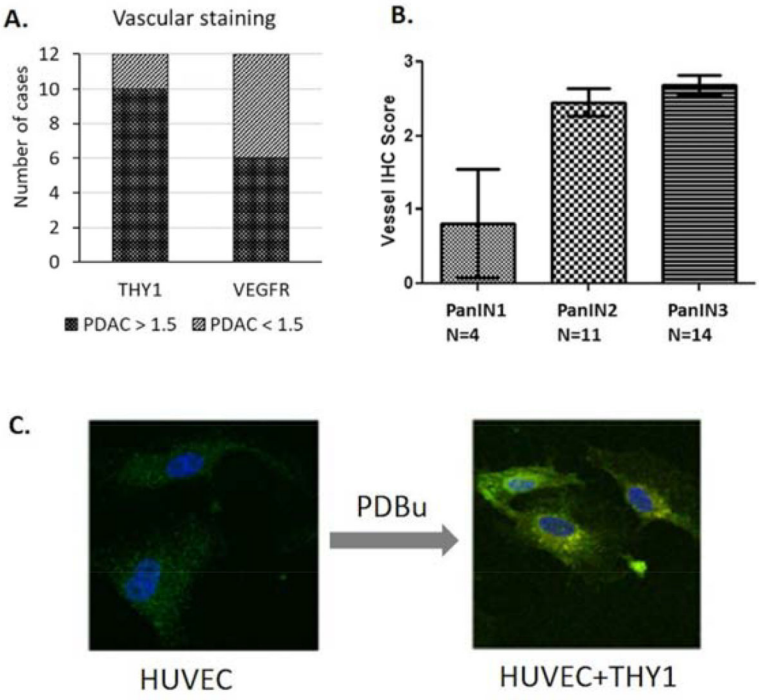

Figure 2.

THY1 expression in PDAC tissues (in comparison to KDR), PanIN lesions and PDBu-stimulated HUVEC cells. A) IHC staining of THY1 and KDR on 12 PDAC tissue slides. The vascular staining of THY1 was positive on 10 out of 12 PDAC samples, whereas the KDR staining was positive on half of the 12 PDAC samples. B) The vascular staining of THY1 was increased substantially in PanIN 2 & 3, compared to PanIN1. C) Florescence images of THY1 expression on HUVEC and PDBu-stimulated HUVEC cells. THY1 expression was visually increased after cancer stimulation by PDBu.

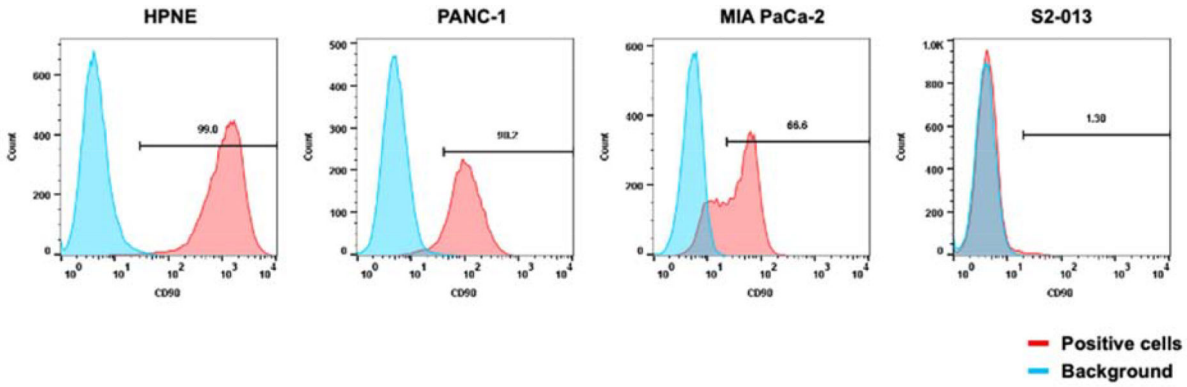

Figure 3.

Level of THY1 expression on various human pancreatic cancer cell lines. Human pancreatic cancer cell lines (HPNE, PANC-1, MIA PaCa-2, and S2–013) were examined for level of THY1 expression using anti-human THY1 antibody. Percentage of positive cells from flow cytometric immunofluorescence histograms is presented.

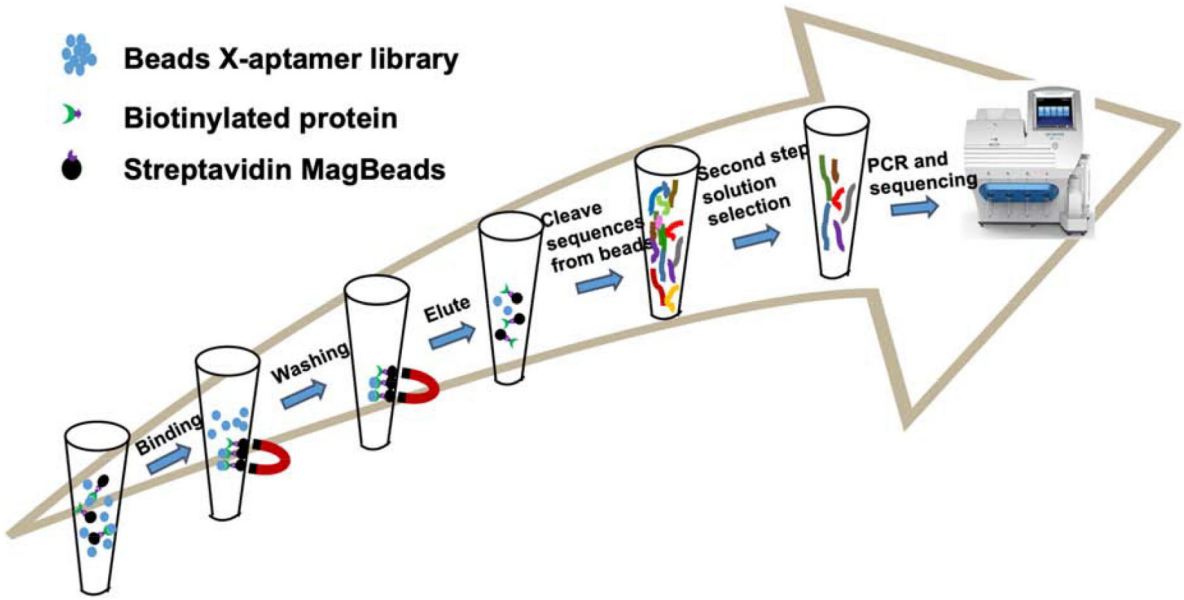

Figure 4.
Scheme of the X-aptamer selection method.

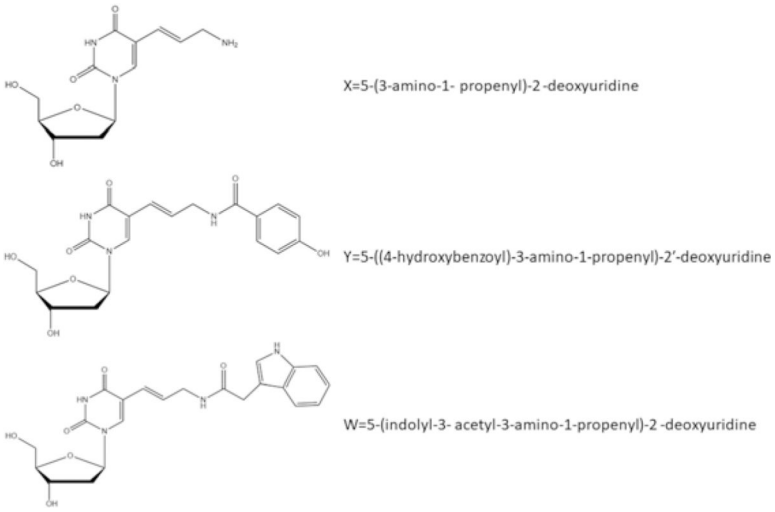

Figure 5.
The structure and linkage chemistry of modifications X, Y, W.

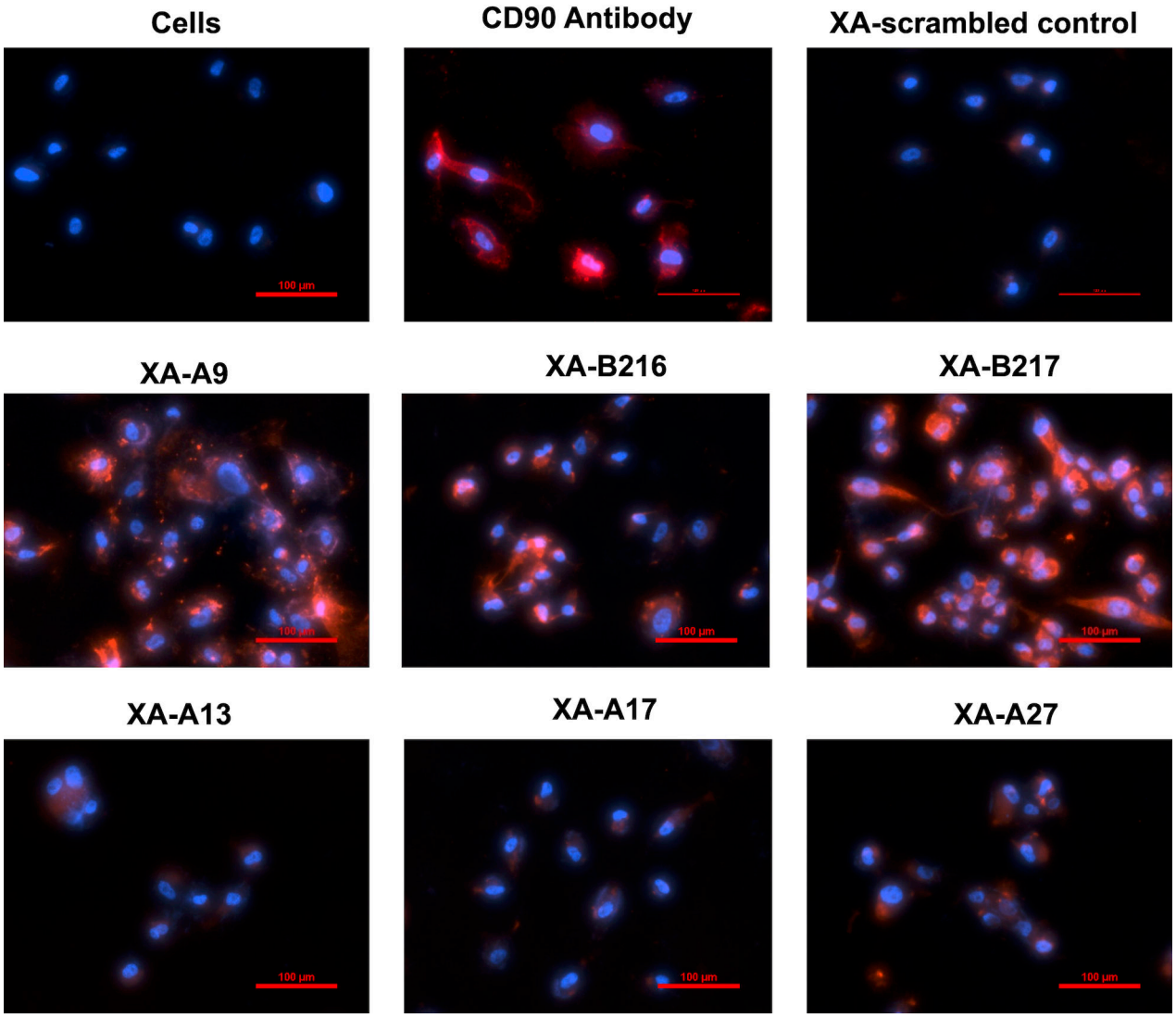

Figure 6.

Screening of binding affinity of individual synthesized XA-THY1s. Biotin conjugated XA-THY1s (500 nM) were incubated with human THY1 expressing HPNE cells. Anti-human THY1 antibody was used as positive control for specific expression of THY1 on HPNE cells. The relative extent of XA binding to the HPNE cells was assessed by fluorescence microscopy analysis using a Nikon Eclipse TE2000-E inverted microscope (Nikon Instruments Inc., Melville, NY). Both XA-THY1s and anti-human THY1 antibody were labeled with red fluorescence. Hoechst 33342 (Thermo Fisher Scientific) was used to counterstain nuclei (blue).

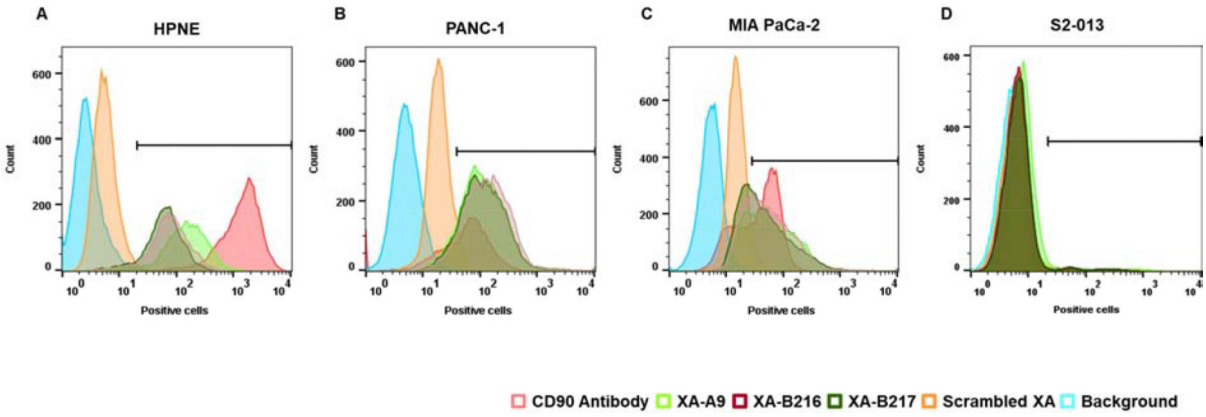

Figure 7.

Binding affinity and specificity of selected XAs. Binding of selected XA-A9, XA-B216 and XA-B217 with various pancreatic cancer cell lines were analyzed by flow cytometry. All three XAs demonstrated high binding affinity and specificity to the THY1 expressing HPNE cells, using the binding activities of THY1 antibody (98%) and scrambled aptamers (1%) as positive and negative control, respectively (A). No binding was observed with THY1 negative pancreatic cancer S2–013 cells with those selected XAs (D). Further validation with other pancreatic cancer cell lines confirmed these selected XAs had similar binding affinity to PANC-1 (B) and MIA PaCa-2 cells (C) compared to THY1 antibody binding.

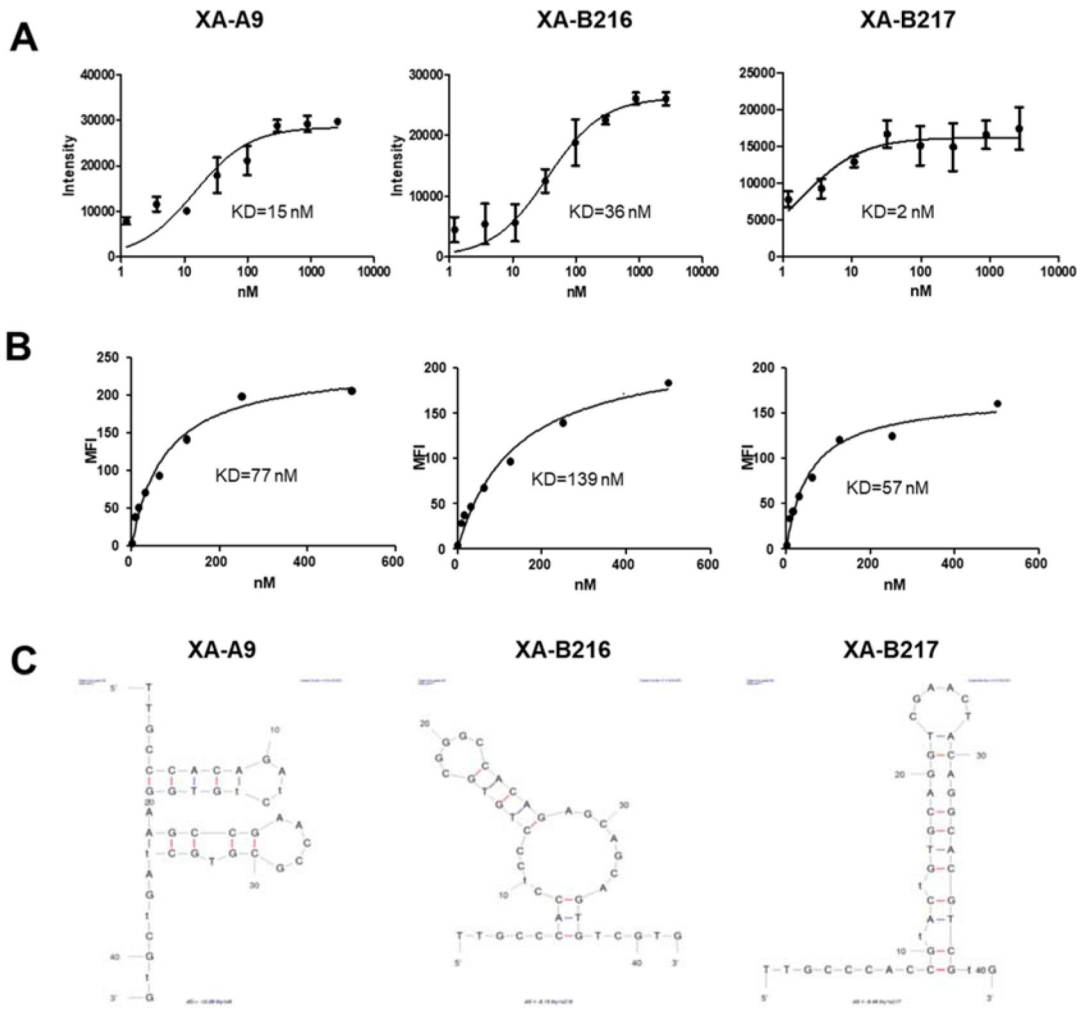

Figure 8.

Binding affinity of selected XAs and their equilibrium dissociation constant. Filter-binding assays were performed with the biotinylated XAs and purified THY1 protein. Saturation binding curves were generated and the equilibrium dissociation constants, Kd, were calculated from the equation Y = Bmax X/(Kd + X), assuming a single binding site (**A)**. Biotin-conjugated THY1 specific XAs were incubated with THY1 expressing HPNE cells at various concentrations and their binding affinity were analyzed by fluorescence intensity with flow cytometry analysis. The equilibrium dissociation constant (Kd) was obtained by fitting the dependence of fluorescence intensity of specific binding on the concentration of the X-aptamers to the equation (B). Secondary structures of the selected XA-A9, XA-B216 and XA-B217 were predicted with the MFold program (C).

Table 1.

NGS selected human THY1 specific X-Aptamers.

Name	Sequence
XA-A9	5’-CAGGGGACGCACCAAGG-TTGCCCACAGAWCYGTGGAAGCCGAACCGCGTGCWAGXCGYG-CCATGACCCGCGTGCTG-3’
XA-B216	5’-CAGGGGACGCACCAAGG-TTGCCCACCYCCCYGTGCGGGCCACAGAGCAGCAGTGXCGYG-CCATGACCCGCGTGCTG-3’
XA-B217	5’-CAGGGGACGCACCAAGG-TTGCCCACCGWACYGTGCAGGXCGAACTACAGGCACGXCGYG-CCATGACCCGCGTGCTG-3’
XA-A13	5’-CAGGGGACGCACCAAGG-TTCACGACXAGACYGTGGCXCCCACAGTCCACCAACGXCGYG-CCATGACCCGCGTGCTG-3’
XA-A17	5’-CAGGGGACGCACCAAGG-TTGCCCACCACACYGTGWWAGXCACAGAYCAACACAGTGGGC-CCATGACCCGCGTGCTG-3’
XA-A27	5’-CAGGGGACGCACCAAGG-TTGCCCACGAACCYGTGGAXCCCACAGAGCGAGCCTGTGGGC-CCATGACCCGCGTGCTG-3’
Scrambled control	5’-CAGGGGACGCACCAAGG-TTGCCCACAGCACYGTGCAXCGCACAGCACGGCAATGTGGGC-CCATGACCCGCGTGCTG-3’

X, Y, W indicate specific modifications at 5-positions of certain uridines on an oligonucleotide backbone. X: amine (lysine). Y: phenol (tyrosine). W: indole (tryptophan).